CellPress

Developmental Cell
Short Article

Vasculature-Associated Cells Expressing Nestin in Developing Bones Encompass Early Cells in the Osteoblast and Endothelial Lineage

Noriaki Ono,[1] Wanida Ono,[1] Toshihide Mizoguchi,[2] Takashi Nagasawa,[3,4] Paul S. Frenette,[2] and Henry M. Kronenberg[1,*]
[1]Endocrine Unit, Massachusetts General Hospital and Harvard Medical School, Boston, MA 02114, USA
[2]Departments of Medicine and of Cell Biology, Ruth L. and David S. Gottesman Institute for Stem Cell and Regenerative Medicine Research, Albert Einstein College of Medicine, Bronx, NY 10461, USA
[3]Department of Immunobiology and Hematology, Institute for Frontier Medical Sciences, Kyoto University, Kyoto 606-8507, Japan
[4]Core Research for Evolutional Science and Technology (CREST), Japan Science and Technology Agency (JST), Tokyo 102-0076, Japan
*Correspondence: hkronenberg@mgh.harvard.edu
http://dx.doi.org/10.1016/j.devcel.2014.03.014

SUMMARY

Nestin-positive (Nes$^+$) cells are important hematopoiesis-supporting constituents in adult bone marrow. However, how these cells originate during endochondral bone development is unknown. Studies using mice expressing GFP under the direction of nestin promoter/enhancer (*Nes*-GFP) revealed distinct endothelial and nonendothelial Nes$^+$ cells in the embryonic perichondrium; the latter were early cells of the osteoblast lineage immediately descended from their progenitors upon Indian hedgehog action and Runx2 expression. During vascular invasion and formation of ossification centers, these Nes$^+$ cells were closely associated with each other and increased in number progressively. Interestingly, cells targeted by tamoxifen-inducible cre recombinase driven by nestin enhancer (*Nes-creER*) in developing bone marrow were predominantly endothelial cells. Furthermore, Nes$^+$ cells in postnatal bones were heterogeneous populations, including a range of cells in the osteoblast and endothelial lineage. These findings reveal an emerging complexity of stromal populations, accommodating Nes$^+$ cells as vasculature-associated early cells in the osteoblast and endothelial lineage.

INTRODUCTION

Bone is a multi-functional organ providing protection for vital organs, levers for motion and withstanding gravity, and the sole site in which hematopoietic stem cells (HSCs) normally generate blood cells in adult mammals. Most bones are formed through endochondral ossification, in which a cartilage template is replaced by bone and bone marrow. During this process, mesenchymal condensations first define the domain for the future bones and then develop into cartilage that continues to grow as chondrocytes proliferate (Kronenberg, 2003). When cells in the central region stop proliferating and become hypertrophic, osteoblasts appear in the surrounding perichondrium (Maes et al., 2010). A population of osteoblast precursors and endothelial cells in the perichondrium coinvades the avascular cartilage and establishes the primary ossification center; osteoblasts and stromal cells then populate the highly vascularized bone marrow. The principal site of hematopoiesis moves from the fetal liver to the spleen and bone marrow during late embryonic development (Christensen et al., 2004). Endochondral ossification establishes an HSC niche de novo within bone marrow (Chan et al., 2009). Marrow stromal cells begin making chemokines, such as chemokine (C-X-C motif) ligand 12 (CXCL12), to support bone marrow hematopoiesis (Nagasawa et al., 1996). A wide range of cells of endochondral bones, including endosteal osteoblasts (Calvi et al., 2003; Zhang et al., 2003), endothelial cells, pericytes (Ding et al., 2012; Sacchetti et al., 2007), and perivascular stromal cells, including CXCL12-abundant reticular cells (Sugiyama et al., 2006), provides micro-environmental cues that maintain hematopoietic stem cells in bone marrow. In adult bone, cells expressing GFP in response to a nestin promoter/enhancer (*Nes*-GFP) and those expressing *Nes-creER* exhibit mesenchymal stem/progenitor activities and constitute an essential HSC niche component (Méndez-Ferrer et al., 2010). Nestin is an intermediate filament protein originally described in neural stem cells and is also expressed in various cell types, including pericytes and nascent endothelial cells, in the developing limb bud and growing tumors (Mokrý et al., 2004; Teranishi et al., 2007; Wroblewski et al., 1997). However, whether similar nestin-expressing cells participate in the process of fetal endochondral ossification and in the formation of cells that support hematopoiesis is unknown. In this study, we sought to identify the origin, heterogeneity, and fate of cells expressing nestin during endochondral bone development. Our data reveal that nestin-expressing cells are associated with vasculature and encompass early cells in the osteoblast, stromal, and endothelial lineages and place nestin expression downstream of Indian hedgehog and Runx2 action in the mesenchymal lineages.

RESULTS

Development of Endothelial and Nonendothelial Nestin$^+$ Cells during Endochondral Ossification

We studied embryonic endochondral bones using *Nes*-GFP mice (Méndez-Ferrer et al., 2010; Mignone et al., 2004). At embryonic day 10.5 (E10.5), Nes$^+$ cells were distributed within the limb bud, partly in a reticular pattern that resembled that of

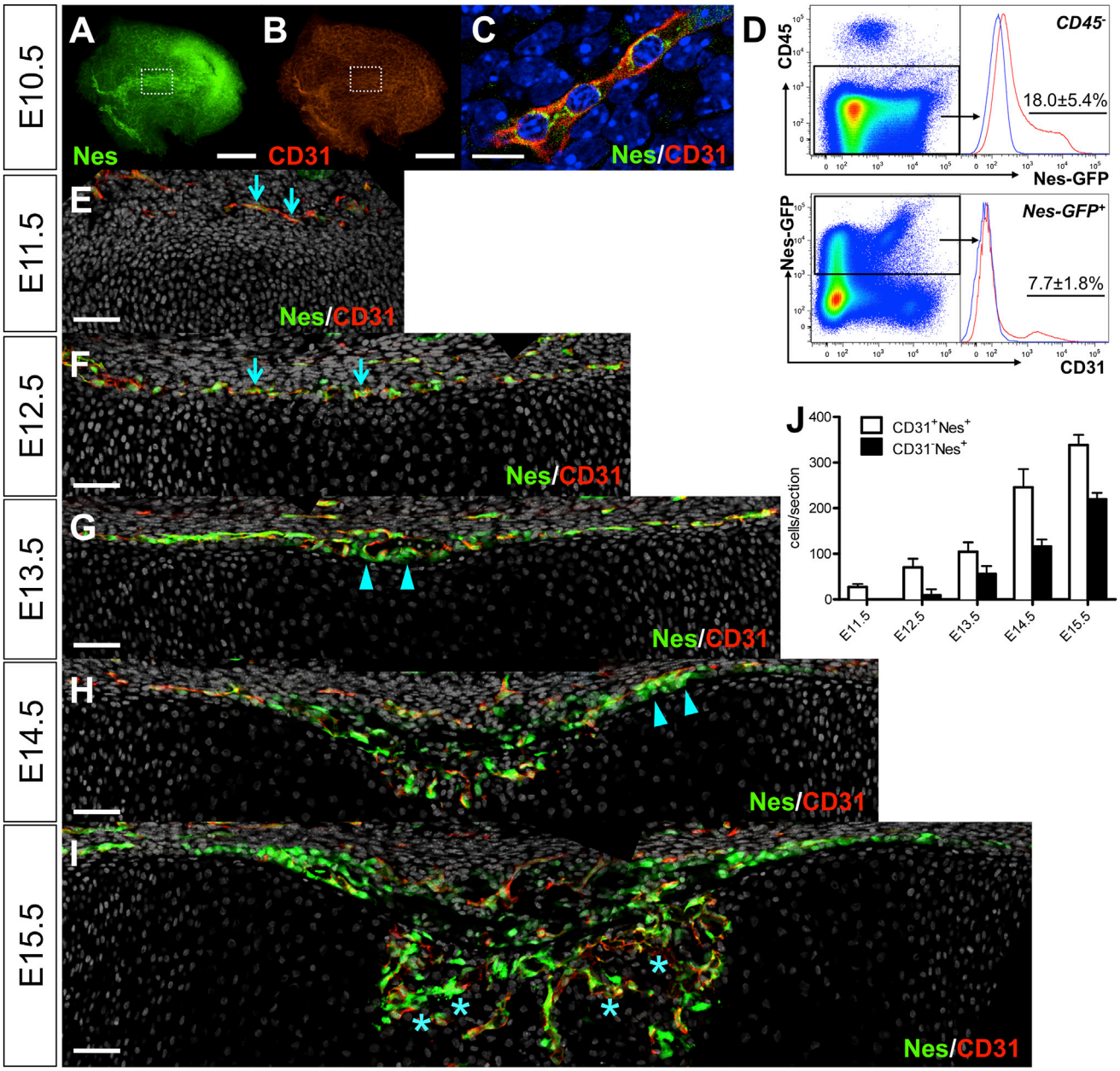

Figure 1. Development of Endothelial and Nonendothelial Nestin+ Cells during Endochondral Ossification

(A–C) E10.5 proximal limb buds of *Nes*-GFP mice were stained whole mount for CD31 and nuclei. In these images, green indicates EGFP signal; red represents Alexa546 signal, and blue represents DAPI signal. (A and B) Images are ×40. (C) Images are ×630 confocal. Scale bars represent 400 μm (A and B) and 10 μm (C). Note that GFP is cytoplasmic and CD31 is membranous.

(D) Flow cytometry analysis of E10.5 *Nes*-GFP limb bud cells stained for CD45 and CD31 (n = 3). Upper panel demonstrates nucleated singlets gated for $CD45^-$; the blue line indicates GFP^- control limb bud cells. Lower panel demonstrates the $CD45^-$ fraction gated for *Nes*-GFP^+; the blue line indicates GFP^+ cells in an unstained control.

(E–I) E11.5–E15.5 femur sections of *Nes*-GFP mice were stained for CD31 and nuclei, and confocal images are shown at ×200 (E–I). Green represents EGFP; red represents Alexa546; and gray represents DAPI. Dorsal halves of growth cartilage are shown. Perichondrium is on top. Arrows point to $CD31^+Nes^+$ cells (E and F). Arrowheads point to $CD31^-Nes^+$ cells in the perichondrium (G and H). Asterisks in vascular invasion front indicate examples of the intimate association of $CD31^+Nes^+$ and $CD31^-Nes^+$ cells (I). Scale bars represent 50 μm.

(J) Quantification of $CD31^+Nes^+$ cells (white bars) and $CD31^-Nes^+$ cells (black bars) in perichondrium and primary ossification center (n = 3–6 per group). All data are represented as mean ± SD.

$CD31^+$ cells, though cells toward the distal end of the limb bud did not show this pattern (Figures 1A and 1B). The reticular Nes^+ cells coexpressed CD31 (Figure 1C). Analysis of dissociated limb bud cells revealed that 18.0% ± 5.4% of $CD45^-$ cells were Nes^+ and 7.7% ± 1.8% of Nes^+ cells were $CD31^+$ (Figure 1D). At E11.5, Nes^+ cells were seldom found within

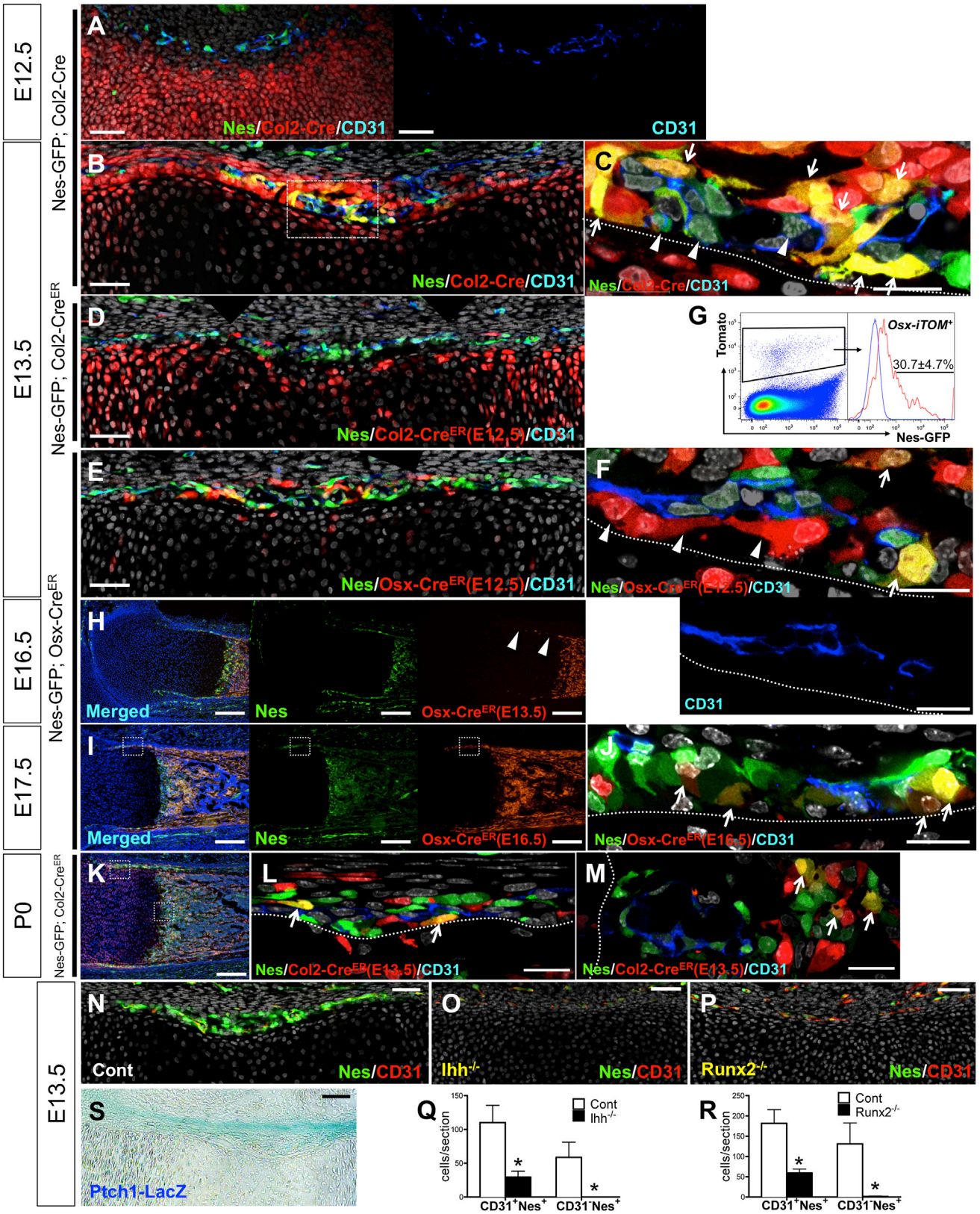

(legend on next page)

mesenchymal condensations, and a small number of CD31$^+$ Nes$^+$ cells were in the area surrounding condensations (Figure 1E, arrows). When the growth cartilage appeared at E12.5, Nes$^+$ cells were found in the perichondrium with large numbers expressing CD31$^+$ (Figure 1F; Figure S1A available online, arrows). At E13.5, a distinct group of CD31$^-$Nes$^+$ cells appeared in the innermost portions of the perichondrium adjacent to the incipient hypertrophic chondrocytes and vasculature (Figure 1G and S1B, arrowheads). At E14.5, both types of Nes$^+$ cells dominated the inner aspect of the enlarging wedge-shaped perichondrium, and CD31$^-$Nes$^+$ cells were aligned on the innermost portion of the flanking perichondrium (Figure 1H, arrowheads). At E15.5, as vascular invasion into the cartilage template occurred, the nascent primary ossification center was populated by both CD31$^+$ and CD31$^-$Nes$^+$ cells that were closely associated with each other (Figure 1I, asterisks; see also Figure S1C). The majority of CD31$^+$ cells found within the perichondrium and the primary ossification center was also Nes$^+$. CD31$^+$Nes$^-$ cells were found mostly outside the bone anlage. The quantification on confocal sections revealed that CD31$^+$Nes$^+$ cells appeared earlier than CD31$^-$Nes$^+$ cells, and both fractions continued to increase as endochondral ossification advanced (Figure 1J). Therefore, these data suggest that distinct endothelial and nonendothelial populations of Nes$^+$ cells are found in the embryonic perichondrium and that these cells closely interact with each other and increase in number during vascular invasion and endochondral ossification.

Nonendothelial Nestin$^+$ Cells Encompass Early Cells of the Osteoblast Lineage

Chondrocytes and chondro-perichondrial progenitors of embryonic endochondral bones express type II collagen (Col2) (Maes et al., 2010; Nakamura et al., 2006; Szabova et al., 2009). To understand how these embryonic progenitors contribute to Nes$^+$ populations, we tracked cell fates using triple-transgenic mice carrying *Nes*-GFP, constitutively active *Col2-cre* (Ovchinnikov et al., 2000), and a *Rosa26* tomato reporter (Madisen et al., 2010). In this system, cells expressing Col2 and their descendants become red, and if they express *Nes*-GFP concurrently, they become yellow. At E12.5, red cells appeared mostly within the growth cartilage and some in the perichondrium and were completely separate from CD31$^+$Nes$^+$ cells (Figure 2A). At E13.5, almost all the CD31$^-$Nes$^+$ cells in the perichondrium were yellow (Figures 2B and 2C, arrows), indicating that they were either expressing Col2 or were descendants of Col2$^+$ cells. In contrast, CD31$^+$Nes$^+$ cells remained green (Figure 2C, arrowheads). To further test if these Nes$^+$ cells themselves express Col2 or descended from Col2-expressing cells, triple-transgenic mice carrying *Nes*-GFP, inducible *Col2-creER* (Nakamura et al., 2006), and a *Rosa26* tomato reporter were generated. These mice received tamoxifen injection at E12.5 and were observed 24 hr later at E13.5. In this paradigm, cells actively expressing Col2 undergo recombination in the presence of tamoxifen and become red. Col2$^+$ cells were seen mostly within the growth cartilage and some in the perichondrium and were completely separate from Nes$^+$ cells (Figure 2D). Furthermore, when mice received tamoxifen at E13.5 and were analyzed 7 days later at P0, descendants of Col2$^+$ cells at E13.5 became yellow in the perichondrium and primary spongiosa (Figures 2K–2M). Therefore, these data suggest that the yellow cells in the perichondrium in Figure 2B are descended from cells, such as the red cells in Figure 2D.

Cells expressing osterix (Osx) in the embryonic perichondrium are osteoblast precursors capable of differentiating into

Figure 2. Nonendothelial Nestin$^+$ Cells Encompass Early Cells of the Osteoblast Lineage

(A–C) *Nes*-GFP; *Col2-cre*; *R26R*^{Tomato} femur sections were stained for CD31 and nuclei, and viewed with confocal microscopy at ×200. (A) Section from E12.5 femur (right panel shows a single color view of CD31 staining). (B) Section from E13.5 femur; shown is confocal image of dotted area at ×630 (C). Arrows point to CD31$^-$Nes$^+$ Tomato$^+$ cells; arrowheads point to CD31$^+$Nes$^+$Tomato$^-$ cells.

(D) *Nes*-GFP; *Col2-creER*; *R26R*^{Tomato} E13.5 femur sections were stained for CD31 and nuclei, and viewed with confocal microscopy at ×200. Pregnant mice received 2 mg tamoxifen at E12.5.

(E and F) *Nes*-GFP; *Osx-creER*; *R26R*^{Tomato} E13.5 femur sections were stained for CD31 and nuclei. Pregnant mice received 2 mg tamoxifen at E12.5. Osteogenic perichondrium is viewed at ×200 in (E) and at ×630 in (F). The lower panel in (F) shows a single color view of CD31 staining. Arrows point to CD31$^-$Nes$^+$ Tomato$^+$ cells; arrowheads point to perivascular Tomato$^+$ cells. Green indicates EGFP; red indicates tdTomato; blue indicates Alexa633; and gray staining indicates DAPI. Scale bars represent 50 μm in (A), (B), (D), and (E) and 20 μm in (C) and (F).

(G) Flow cytometry analysis of E13.5 *Nes*-GFP; *Osx-creER*; *R26R*^{Tomato} limb cells after administration of tamoxifen at E12.5 and staining for CD45. The CD45$^-$ fraction was gated for Tomato$^+$; the blue line indicates the pattern of *Nes*-GFP$^-$Tomato$^+$ limb cells (n = 3).

(H) *Nes*-GFP; *Osx-creER*; *R26R*^{Tomato} E16.5 femur sections were viewed at ×100 after administration of tamoxifen at E13.5 and stained for nuclei. Arrowheads point to Tomato$^+$ cells disappearing from the osteogenic perichondrium. Green indicates EGFP; red indicates tdTomato; and blue represents DAPI.

(I and J) *Nes*-GFP; *Osx-creER*; *R26R*^{Tomato} E17.5 femur sections were viewed after administration of tamoxifen at E16.5. In (I) they were stained for CD31 and nuclei and viewed at ×100. In (J) the confocal image was viewed at ×630. Arrows point to CD31$^-$Nes$^+$Tomato$^+$ cells on the innermost layer of the osteogenic perichondrium. Scale bars represent 200 μm in (H) and (I) and 50 μm in (J).

(K–M) *Nes*-GFP; *Col2-creER*; *R26R*^{Tomato} P0 femur sections were viewed after administration of tamoxifen at E13.5 and stained for CD31 and nuclei. (K) is shown at ×100. (L) is a confocal image of perichondrium, delineated by dotted line and shown at ×630; (M) is a confocal image of primary spongiosa, delineated by dotted line. Arrows point to CD31$^-$Nes$^+$ Tomato$^+$ cells. Green indicates EGFP; red indicates tdTomato; blue indicates Alexa633; and gray indicates DAPI. Scale bars represent 200 μm for (K) and 20 μm for (L) and (M).

(N–P) E13.5 femur sections were stained for CD31 and nuclei. Section from a control mouse is shown in (N), from an Ihh$^{-/-}$ mouse in (O), and from a Runx2$^{-/-}$ mouse in (P). All are confocal images at ×200. Green indicates EGFP; red indicates Alexa546; and gray indicates DAPI. Scale bars represent 50 μm.

(Q) Quantification of CD31$^+$Nes$^+$ cells and CD31$^-$Nes$^+$ cells in perichondrium. Control cells are shown in white bars, and Ihh$^{-/-}$ cells are shown in black bars. n = 4 per group, *p < 0.05.

(R) Quantification of CD31$^+$Nes$^+$ cells and CD31$^-$Nes$^+$ cells in perichondrium. Control cells are shown in white bars, and Runx2$^{-/-}$ cells are shown in black bars. n = 4 per group, *p < 0.05.

(S) Ptch1$^{LacZ/+}$ femur from E13.5 mice was stained for β-galactosidase activity and shown at ×200. Scale bar represents 50 μm.

All data are represented as mean ± SD.

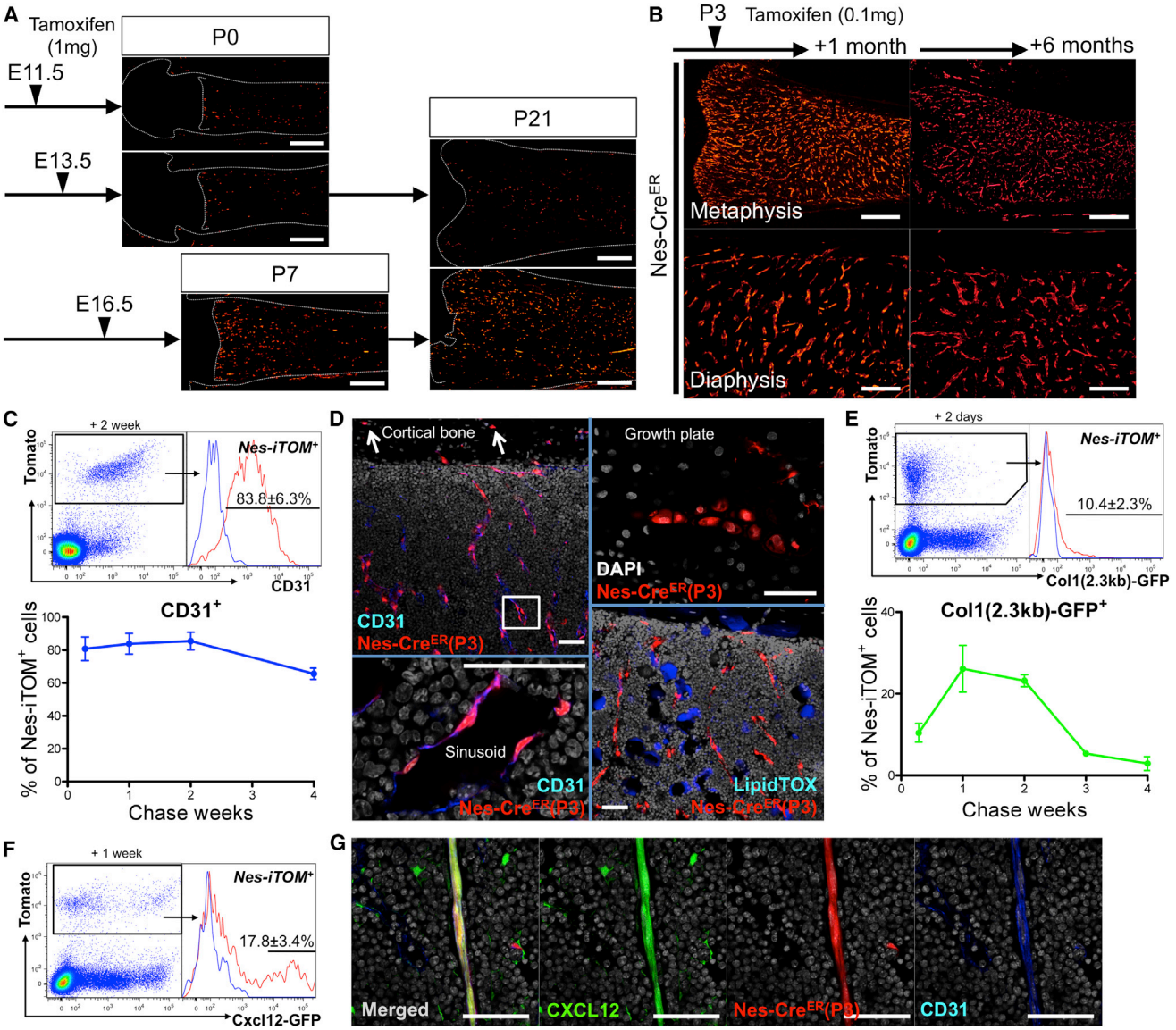

Figure 3. *Nes-creER* Preferentially Targets Nestin+ Endothelial Cells in Developing Bone Marrow

(A) Pregnant mice received 1 mg tamoxifen at indicated points (E11.5, E13.5, or E16.5), and *Nes-creER*; *R26R*^{Tomato} mice were chased until the indicated postnatal day (P0, P7, or P21). Distal femur sections are shown at ×40. Red indicates tdTomato. Scale bars represent 500 μm.

(B) *Nes-creER*; *R26R*^{Tomato} mice received 0.1 mg tamoxifen at P3 and were chased for 1 month (left panels) and 6 months (right panels). Upper panels show distal femur and metaphysis at ×40. Scale bars indicate 500 μm; lower panels show diaphysis at ×100. Scale bars represent 200 μm. Red indicates tdTomato.

(C) Flow cytometry analysis of epiphyseal/metaphyseal cells from *Nes-creER*; *R26R*^{Tomato} mice that received tamoxifen at P3 and were chased for indicated periods. Cells were stained for CD45 and CD31. The upper panel shows CD45$^-$ fraction after 2 weeks of chase, gated for Tomato$^+$. The blue line indicates the tracing for Tomato$^+$ cells from an unstained control. The lower panel shows the percentage of CD31$^+$ cells within the CD45$^-$Tomato$^+$ fraction when mice were chased for 2 days (n = 4), 1 week (n = 6), 2 weeks (n = 2), and 4 weeks (n = 4).

(D) *Nes-creER*; *R26R*^{Tomato} were given tamoxifen at P3, and femur sections were examined. Left panels show diaphysis after 1 month of chase stained for CD31 and nuclei. Upper left is a confocal image at ×200. Arrows indicate Tomato$^+$ osteocytes in cortical bone. Lower left is a confocal image (at ×630) of the boxed area from the upper left, rotated perpendicularly, revealing a bone marrow sinusoid. Red indicates tdTomato; blue indicates Alexa633; and gray indicates DAPI. Upper right panel shows a confocal image (×400) of growth plate cartilage after 2 months of chase. Note Tomato$^+$ columnar chondrocytes. Red indicates tdTomato, and gray indicates DAPI. Lower right panel is a confocal image at ×200, showing diaphysis after 4 months of chase, stained for lipid. Red indicates tdTomato, and blue indicates LipidTOX Deep Red. Scale bars represent 50 μm.

(E) Flow cytometry analysis of epiphyseal/metaphyseal cells from *Col1(2.3kb)*-GFP; *Nes-creER*; *R26R*^{Tomato} mice. The mice received tamoxifen at P3 and were chased for the indicated periods. Cells were stained for CD45. Upper panel shows the CD45$^-$ fraction after 2 days of chase, gated for Tomato$^+$. The blue line represents Tomato$^+$ cells in an unstained control. Lower panel shows the percentage of *Col1(2.3kb)*-GFP$^+$ cells within the CD45$^-$Tomato$^+$ fraction after the mice were chased for 2 days (n = 4), 1 week (n = 5), 2 weeks (n = 2), 3 weeks (n = 4), and 4 weeks (n = 4).

(legend continued on next page)

osteoblasts, osteocytes, and peritrabecular stromal cells (Maes et al., 2010). To understand how Nes+ cells are related to osterix-expressing precursors, triple transgenic mice carrying *Nes*-GFP, inducible *Osx-creER*, and *Rosa26* tomato reporter received tamoxifen at E12.5 and were analyzed 24 hr later at E13.5. At E13.5, a great majority of red cells was found in the perichondrium (Figure 2E), and some of these cells overlapped with CD31−Nes+ cells and became yellow in the perichondrium (Figure 2F, arrows). In addition, these red cells were closely associated with, but clearly independent from, CD31+Nes+ cells (Figure 2F, arrowheads). Analysis of dissociated limb cells revealed that 30.7% ± 4.7% of red cells expressed *Nes*-GFP (Figure 2G). Furthermore, when mice received tamoxifen at E13.5 and were analyzed at E16.5, a large majority of descendants of osterix-expressing cells at E13.5 moved into the primary ossification center and did not stay in the newly generated part of the perichondrium (Figure 2H, arrowheads). These red cells completely disappeared from the perichondrium when chased until postnatal day 0 (data not shown). When mice received tamoxifen at E16.5 and were observed 24 hr later at E17.5, the domain of red cells extended over the Nes+ perichondrium (Figure 2I). In fact, many yellow cells were observed on the inner aspect of the perichondrium (Figure 2J, arrows), indicating that these CD31−Nes+ perichondrial cells expressed osterix. Thus, at least some CD31−Nes+ cells in the perichondrium are Osx+ osteoblast precursors that are continually replenished from their precursors as bones become longer.

Runx2 is an essential regulator of osteoblast differentiation downstream of Indian hedgehog (Ihh), as *Runx2* mRNA is absent from the perichondrium in the absence of Ihh (St-Jacques et al., 1999). The Ihh receptor, Patched1, is a direct Ihh target gene. In *Ptch1*-LacZ knockin mice, robust β-galactosidase activities were observed in the perichondrium at E11.5 (data not shown) and E13.5 (Figure 2S), demonstrating Ihh action in the perichondrium. To determine the role of Ihh signaling in *Nes*-GFP cells, double-transgenic mice carrying *Nes*-GFP and Ihh null alleles were analyzed at E13.5. The number of CD31+ Nes+ cells was significantly reduced and CD31−Nes+ cells were completely abrogated in the resultant thin perichondrium (Figures 2O and 2Q). Runx2 deficiency also significantly reduced the number of CD31+Nes+ cells and led to complete loss of CD31−Nes+ cells in the perichondrium at E13.5 (Figures 2P and 2R). No CD31−Nes+ cells were observed in Runx2-deficient perichondrium when bones developed further at E16.5 and E18.5 (data not shown). Thus, Ihh and Runx2 are required for generating nonendothelial Nes+ cells in the perichondrium during embryonic endochondral bone development. In addition, Ihh and Runx2 are also important for endothelial Nes+ cells in the perichondrium, and disappearance of CD31−Nes+ cells in Ihh null or Runx2 null embryos is likely to occur through a combination of cell-autonomous and non-cell-autonomous effects.

These data indicate that Ihh and Runx2 both are needed to direct mesenchymal precursors to become Nes+ cells of the osteoblast lineage in the perichondrium; some of these cells become Osx+ preosteoblasts.

Nes-creER Preferentially Targets Nestin+ Endothelial Cells in Developing Bone Marrow

In order to unravel the fate of Nes+ cells at different stages of endochondral ossification, we took advantage of mice expressing an inducible Cre recombinase under the control of a minimal promoter and a 1.8 kb nestin second intron enhancer (*Nes-creER*) (Balordi and Fishell, 2007), along with a *Rosa26* tomato reporter. When mice received tamoxifen before the primary ossification center was formed, either during formation of condensations at E11.5 or of the osteogenic perichondrium at E13.5, only a small number of red cells was observed in bone upon chase until the day of birth (P0) or until postnatal day 21 (P21). When mice received tamoxifen at E16.5 at the time that the marrow space starts to form, larger numbers of red cells appeared in bone, when chased until P7 or P21 (Figure 3A). Therefore, there appears to be a transition of *Nes-creER* expression before and after the primary ossification center is established. To delineate the fate of *Nes-creER*-targeted cells after bone marrow hematopoiesis is fully established, mice received tamoxifen at postnatal day 3 (P3). Descendants of these cells [Nes-creER(P3)] continued to dominate the entire bone marrow up to the border with the growth plate, in a reticular pattern similar to marrow vasculature for at least 6 months thereafter (Figure 3B). Analysis of dissociated cells from the epiphysis and metaphysis revealed that a majority of Nes-creER(P3) cells were consistently positive for CD31 for the entire first month of chase (Figure 3C). Histological analysis revealed that Nes-creER(P3) red cells were predominantly sinusoidal endothelial cells in bone marrow (Figure 3D, left panels). In contrast, only a small number of Nes-creER(P3) cells became red osteoblasts and osteocytes in the cortical bone (Figure 3D, arrows; see also Figure S2A), and very infrequently became chondrocytes in the growth plate (Figure 3D, right upper panel). Further, Nes-creER(P3) cells did not become adipocytes (Figure 3D, right lower panel). To understand the contribution of Nes-creER(P3) cells to osteoblastic cells, triple transgenic mice carrying *Col1(2.3kb)*-GFP, *Nes-creER*, and a *Rosa26* tomato reporter were generated and received tamoxifen at P3. Analysis of dissociated bone cells revealed that 10.4% ± 2.3% of Nes-creER(P3) cells were osteoblasts expressing GFP at 48 hr after injection; this increased to 26.1% ± 5.7% and 23.2% ± 1.5% for the first and second weeks and then decreased to 5.4% ± 0.1% and 2.9% ± 1.7% for the third and fourth weeks, respectively (Figure 3E; see also Figure S2B for images).

Various types of cells in bone and bone marrow express CXCL12, a crucial chemokine for maintaining hematopoietic stem cells (HSCs) (Nagasawa et al., 1996), whereas depletion of *Nes-creER* cells rapidly reduces HSCs (Méndez-Ferrer et al., 2010). To understand how *Nes-creER* cells contribute to CXCL12-expressing cells, triple-transgenic mice carrying *Cxcl12*-GFP (Ara et al., 2003), *Nes-creER*, and a *Rosa26* tomato reporter were generated and received tamoxifen at P3. After a

(F and G) Flow cytometry analysis of epiphyseal/metaphyseal cells from *Cxcl12*-GFP; *Nes-creER*; *R26R*^{Tomato} mice that received tamoxifen at P3 and were chased for 1 week. (F) The CD45− fraction gated for Tomato+ (n = 6) is shown. The blue line indicates a trace of *Cxcl12*-GFP−Tomato+ cells. (G) Sections of the bone marrow of the femoral diaphysis were viewed with confocal images at ×630 after stained for CD31 and nuclei. Green staining indicates EGFP; red staining indicates tdTomato; blue staining indicates Alexa633; and gray staining indicates DAPI. Scale bars, represent 50 μm. All data are represented as mean ± SD.

week of chase, 17.8% ± 3.4% of Nes-creER(P3) cells were *Cxcl12*-GFP$^+$ (Figure 3F), and Nes-creER(P3) endothelial cells of the arterioles were found to be *Cxcl12*-GFP$^+$; some of the Nes-creER cells were stromal cells as well (Figure 3G; see also Figures S2C and S2D for images).

These data suggest that *Nes-creER* predominantly marks cells that become endothelial cells and cells that become osteoblasts, osteocytes, stromal cells, and chondrocytes.

Nestin$^+$ Cells in Developing Postnatal Bones Are Heterogeneous Stromal Cell Populations

In postnatal endochondral bones at 1 week of age, the *Nes*-GFP signal was particularly intense in two locations: perivascular cells in the primary spongiosa immediately adjacent to the growth plate (Figure 4A, left panel, arrows) and pericytes of the arterioles (Figure 4A, arrowheads; see Figure 4C below). In addition, a moderate *Nes*-GFP signal was found in osteoblasts on the bone surface, osteocytes (Figure 4A, asterisks; see also Figure S3), and endothelial cells (Figure 4C, asterisks). In adult endochondral bones at 2 months of age, the number of *Nes*-GFP^{hi} cells was decreased in the primary spongiosa and bone marrow (Figure 4B, left panel, arrows). *Nes*-GFP^{lo} cells in osteoblasts on bone surfaces and osteocytes were also decreased but still observed (Figure 4B, left panel, asterisks, right panel, arrowheads; see also Figure S3). To delineate the difference between cell types that *Nes*-GFP and *Nes-creER* differentially target, mice carrying both of these transgenes were generated, received tamoxifen at P3, and analyzed 48 hr later. A large majority of red cells targeted by *Nes-creER* was found to be CD31$^+$ endothelial cells in the primary spongiosa and bone marrow (Figure 4C, asterisks). Analysis of dissociated bone cells revealed that almost all the *Nes-creER*-tomato cells were also *Nes*-GFP positive (Figure 4D, left panel). However, whereas 33.7% ± 7.0% of *Nes*-GFP cells were CD31$^+$, 80.8% ± 7.2% of *Nes-creER*-tomato cells were CD31$^+$ (Figure 4D, right panels), suggesting that *Nes-creER* preferentially targets an endothelial subpopulation of Nes$^+$ cells. To study if cells expressing *Nes*-GFP and/or *Nes-creER*-tomato actually express nestin gene, we examined Nestin immunoreactivity and the expression of *Nestin* mRNA in these cell populations (Figures S3E–S3K). These data confirm that cells expressing these transgenes also express nestin mRNA and protein. To delve more into the heterogeneity of Nes$^+$ cells in postnatal bones, *Nes*-GFP was combined with cre lines targeting distinct stromal cell lineages: *Osx-cre* for osteoblasts (Rodda and McMahon, 2006), *Tie2-cre* for endothelial cells, and *LepR-cre* for perivascular stromal cells (Ding et al., 2012). At P3 (*Tie2-cre*) or P7 (*Osx-cre*, *LepR-cre*), 97.7% ± 0.7% of *Osx-cre*, 94.3% ± 2.9% of *Tie2-cre*, and 97.2% ± 0.5% of *LepR-cre*-targeted CD45$^-$ cells were positive for *Nes-GFP* (Figure 4E). To focus further on osteoblast subpopulations of Nes$^+$ cells, *Nes*-GFP was combined with creER^{T2} lines targeting different stages of the osteoblast lineage (*Osx-creER*, *Col1(3.2kb)-creER* and *osteocalcin (Ocn)-creER*). After a pulse at P3, followed by 1 week of chase, 95.7% ± 4.8%, 91.8% ± 4.5%, and 92.9% ± 1.5% of cells targeted by *Osx-creER*, *Col1(3.2kb)-creER*, and *Ocn-creER*, respectively, were positive for *Nes-GFP* (Figure 4F). Therefore, inasmuch as these reporter lines are specific for their respective lineages, Nes$^+$ cells include a wide range of cells in the endothelial, stromal, and osteoblast lineage.

DISCUSSION

Establishment of hematopoiesis and bone formation within the bone marrow during embryonic endochondral ossification requires an orchestrated invasion of osteoblast precursors and endothelial cells from the perichondrium into the avascular cartilage. Many cell types putatively supporting hematopoietic stem cells in bone marrow, e.g., osteoblasts, stromal cells, pericytes, and endothelial cells, are generated simultaneously as the primary ossification center forms. Our data indicate that nestin$^+$ cells during this process are associated with vasculature and include both endothelial and nonendothelial cells. We used two different "nestin" constructs, both containing an intronic enhancer sequence: one uses a *nestin* gene promoter to drive GFP expression (Mignone et al., 2004), whereas the other uses a minimal promoter to drive *creER* expression (Balordi and Fishell, 2007). We found that the two constructs mark both endothelial and mesenchymal cell types, with the latter marking a higher proportion of endothelial cells in fetal and early postnatal life.

Méndez-Ferrer et al. (2010) showed that, in adult bone marrow, *Nes*-GFP$^+$ cells include all cells capable of forming CFU-F colonies in vitro; these colonies form from single cells and can generate osteoblasts, chondrocytes, and adipocytes in vitro. Also, they showed that *Nes-creER*-targeted cells in adult marrow could become osteoblasts, osteocytes, and chondrocytes in vivo and were also required to support hematopoiesis. We used a series of cell-type-specific transgenes and mutant mice to order the expression of the nestin transgenes in fetal bone. We found that neither of these transgenes was expressed in mesenchymal condensations. *Nes*-GFP was expressed in endothelial and nonendothelial cells in the perichondrium. The latter cells appeared downstream of cells expressing transgenes driven by the type II collagen promoter: *Col2-cre*-tomato reporter marked chondrocytes and perichondrial cells distinct from cells expressing *Nes*-GFP$^+$ at E12.5. Similarly, when *Col2-creER* mice were given tamoxifen at E12.5 and examined at E13.5, the marked cells were distinct from cells expressing *Nes*-GFP. When similar mice given tamoxifen at E13.5 were examined at P0, many *Nes*-GFP$^+$ cells were descended from those expressing *Col2-creER* at E13.5. These findings allow us to place *Nes*-GFP expression downstream of *Col2-creER* expression in the lineage of fetal perichondrial cells.

It is of interest that, in fetal life, neither nestin construct marks the mesenchymal condensations that give rise to chondrocytes and osteoblasts; they appear in the perichondrium only after Col2$^+$ cells populate there. Thus, multi-lineage potential is not solely a property of the earliest cells of the osteoblast lineage during development. Further, because osteoblasts and bone lining cells are also Nes$^+$ (Figures 4A and 4B; Figure S3), it is unlikely that all Nes$^+$ cells are multipotent in normal development.

Mice with the Ihh gene ablated fail to form osteoblasts in limb perichondrium (St-Jacques et al., 1999). We found that these mice also fail to generate perichondrial cells expressing *Nes*-GFP. Mice with the Runx2 gene ablated fail to form osteoblasts (Otto et al., 1997), and these mice fail to generate perichondrial cells expressing *Nes*-GFP. Thus, perichondrial CD31$^-$*Nes*-GFP$^+$ cells require both Ihh and Runx2 expression and also appear after expression of the *Col2-cre* transgene. In contrast,

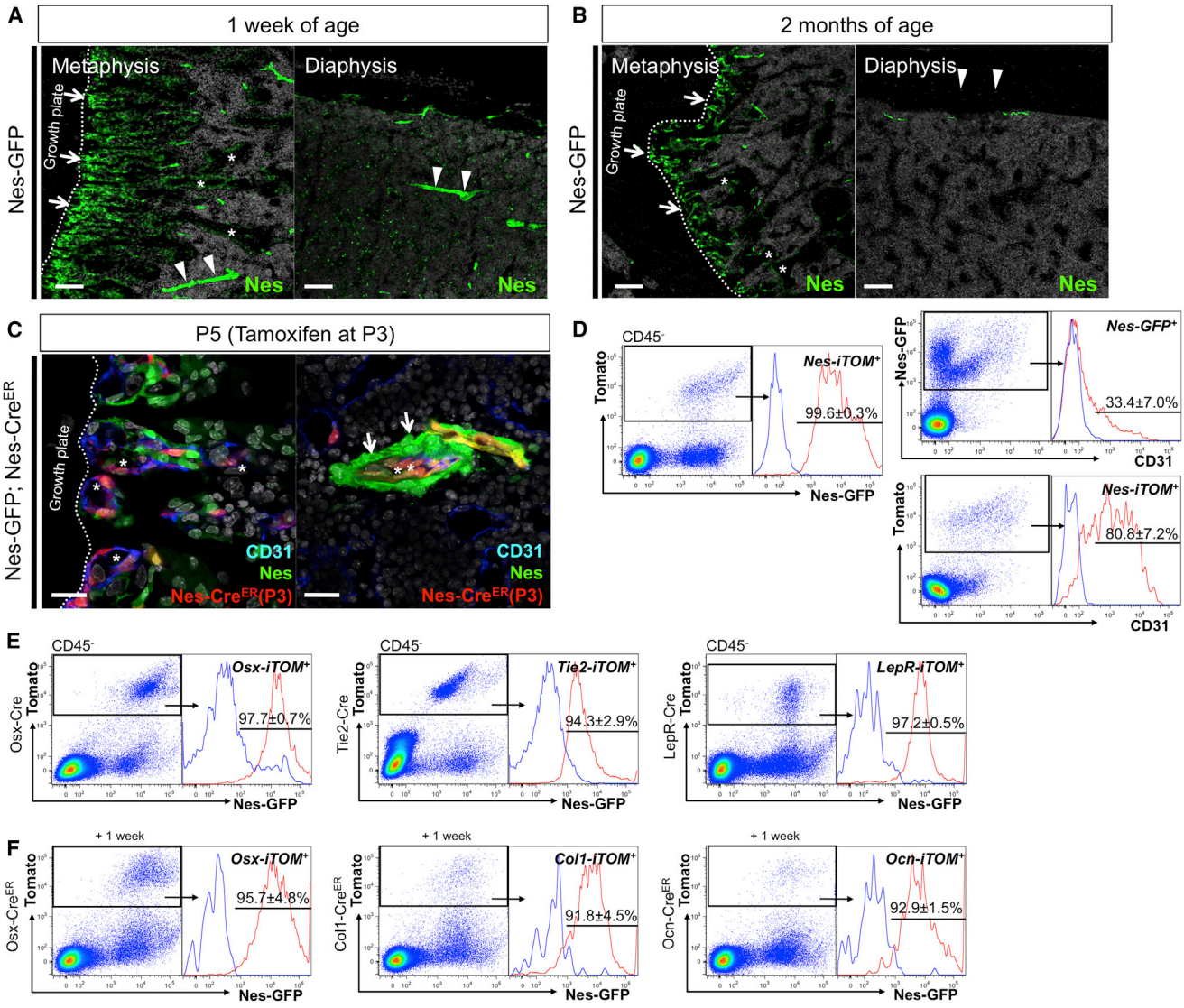

Figure 4. Nestin+ Cells in Developing Postnatal Bones Are Heterogeneous Stromal Cell Populations

(A and B) Distal femur sections of *Nes*-GFP mice at (A) 1 week of age and (B) 2 months of age were stained for nuclei. Confocal images at ×100 of metaphysis (left panels) and diaphysis (right panels) are shown. Arrows indicate *Nes*-GFP^{hi} cells in the primary spongiosa adjacent to the growth plate. Arrowheads in (A) point to pericytes of bone marrow arterioles; asterisks indicate osteoblasts on the bone surface and osteocytes. Arrowheads in (B) point to osteocytes in cortical bone. Scale bars represent 100 μm.

(C and D) *Nes*-GFP; *Nes-creER*; *R26R*^{Tomato} mice received tamoxifen at P3 and were chased for 48 hr. (C) Femur sections of metaphysis (left panel) and diaphysis bone marrow (right panel) were stained for CD31 and nuclei and viewed with confocal microscopy at ×630. Asterisks indicate CD31$^+$Tomato$^+$ cells. Arrows point to pericytes of bone marrow arterioles. Green indicates EGFP; red represents tdTomato; blue represents Alexa633; and gray represents DAPI. Scale bars represent 20 μm. (D) Flow cytometry analysis of epiphyseal/metaphyseal cells stained for CD45 and CD31. CD45$^-$ fraction gated for Tomato$^+$ (left panel and lower right panel) and *Nes*-GFP$^+$ (upper right panel) (n = 4); blue line: *Nes*-GFP$^-$Tomato$^+$ cells (left panel) and unstained controls (right panels).

(E) Flow cytometry analysis of epiphyseal/metaphyseal cells from *Nes*-GFP; *R26R*^{Tomato} mice that also carry *Osx-cre* (left panel), *Tie2-cre* (center panel), or *LepR-cre* (right panel). Cells were harvested at P3 (*Tie2-cre*) or P7 (*Osx-cre, LepR-cre*).

(F) Flow cytometry analysis of epiphyseal/metaphyseal cells from *Nes*-GFP; *R26R*^{Tomato} mice that also carry *Osx-creER* (left panel), *Col1-creER* (center panel), or *Ocn-creER* (right panel). Tamoxifen was administered at P3 and cells were harvested a week later. The CD45$^-$ fraction was gated for Tomato$^+$. For *Osx-cre* cells, n = 3; for *Tie2-cre* cells, n = 4; for *LepR-cre* cells, n = 3, for *Osx-creER* cells, n = 6; for *Col1-creER* cells, n = 4; and for *Ocn-creER* cells, n = 3. The blue lines represent a GFP$^-$ control. All data are represented as mean ± SD.

when *Osx-creER* is activated at E12.5, many CD31$^-$*Nes*-GFP$^+$ cells at E13.5 expressed the tomato reporter. Similarly, when *Osx-creER* is activated at later times, expression of the tomato reporter largely overlaps with expression of *Nes*-GFP. Also, both *Col1-creER* and *Ocn-creER* marked a subset of *Nes*-GFP$^+$ cells. Thus, the CD31$^-$*Nes*-GFP$^+$ cells appear roughly at the time of Osx expression, and *Nes*-GFP transgene remains active in subsequent cells of the osteoblast lineage.

Nes-creER directs reporter expression in nonendothelial stromal cells in the marrow, and *LepR-cre* also directs expression in *Nes*-GFP$^+$ cells; thus, stromal cells represent one fate for nestin-expressing cells. In the accompanying manuscript, Mizoguchi et al. (2014; this issue of *Developmental Cell*) show that postnatally marked cells expressing *Nes*-GFP and *Osx-creER*-tomato include stromal cells with properties of "mesenchymal stem/progenitor cells."

Endosteal osteoblasts, endothelial cells, pericytes, and perivascular stromal cells have been implicated in defining the hematopoietic stem cell niche in bone marrow (Ding et al., 2012; Ding and Morrison, 2013; Greenbaum et al., 2013). Our data indicate that all these cell types in developing bone marrow express *Nes*-GFP. We also found that *Nes-creER* predominantly targets endothelial cells in bone marrow, including Cxcl12$^+$ endothelial cells of the bone marrow arteriole (Figure 3G). Our findings support the notion that both endothelial and nonendothelial Nes$^+$ cells are important components of the hematopoietic stem cell niche.

EXPERIMENTAL PROCEDURES

Mice

Nestin-GFP, Col2a1-cre, Osx-cre, Col2a1-creER^{T2}, Osx-creER^{T2}, Col1-creER^{T2}, Ocn-creER^{T2}, Ihh-Neo/null, Runx2-LacZ/null, Ptch1-LacZ/null, and Cxcl12-GFP/null mice have been described elsewhere. Tie2-cre (JAX8863), LepR-cre (JAX8320), and Rosa26-loxP-stop-loxP-tdTomato (R26R-tomato, JAX7914) were acquired from Jackson Laboratory. All procedures were conducted in compliance with the Guideline for the Care and Use of Laboratory Animals approved by Massachusetts General Hospital's Institutional Animal Care and Use Committee (IACUC). For embryonic experiments, male mutant mice were mated to female CD1 mice, and the vaginal plug was checked in the morning. Pregnant mice received 1 mg tamoxifen (Sigma T5648) and progesterone (Sigma P3972) intraperitoneally (i.p.). For postnatal experiments, 3-day-old mice received 0.1 mg of tamoxifen i.p. Tamoxifen was dissolved first in 100% ethanol and then in sunflower seed oil (Sigma S5007) overnight at 60°C.

Histology and Flow Cytometry

Frozen sections at 15 μm thickness were analyzed using a fluorescence (Nikon Eclipse E800) or a confocal (Zeiss LSM510) microscope. Enzymatically digested cells from dissected femurs and tibias were stained for anti-mouse CD45-APC, CD31-eFlour 450 (1:500, eBioscicence) and analyzed using a four-laser BD LSRII flow cytometer. More detailed experimental procedures are available in the Supplemental Experimental Procedures.

Statistical Analysis

Results were represented as mean values ± SD. Statistical evaluation was conducted based on Mann-Whitney's *U*-test. A p value of <0.05 was considered significant.

SUPPLEMENTAL INFORMATION

Supplemental Information includes Supplemental Experimental Procedures and three figures and can be found with this article online at http://dx.doi.org/10.1016/j.devcel.2014.03.014.

ACKNOWLEDGMENTS

The authors thank Andrew McMahon for *Ptch1*-LacZ and *Ihh*-null mice and David Rowe for *Col2.3*-GFP mice. This work was supported by grants from the National Institutes of Health (DE022564 to N.O., DK056638 and HL069438 to P.S.F., and DK056246 to H.M.K.) and the Gideon & Sevgi Rodan fellowship from the International Bone & Mineral Society and the Japan Society for the Promotion of Science Fellowship for Research Abroad and Grant-in-Aid for Young Scientists (21689051) (to N.O.).

Received: August 24, 2013
Revised: January 12, 2014
Accepted: March 18, 2014
Published: May 12, 2014

REFERENCES

Ara, T., Tokoyoda, K., Sugiyama, T., Egawa, T., Kawabata, K., and Nagasawa, T. (2003). Long-term hematopoietic stem cells require stromal cell-derived factor-1 for colonizing bone marrow during ontogeny. Immunity *19*, 257–267.

Balordi, F., and Fishell, G. (2007). Mosaic removal of hedgehog signaling in the adult SVZ reveals that the residual wild-type stem cells have a limited capacity for self-renewal. J. Neurosci. *27*, 14248–14259.

Calvi, L.M., Adams, G.B., Weibrecht, K.W., Weber, J.M., Olson, D.P., Knight, M.C., Martin, R.P., Schipani, E., Divieti, P., Bringhurst, F.R., et al. (2003). Osteoblastic cells regulate the haematopoietic stem cell niche. Nature *425*, 841–846.

Chan, C.K., Chen, C.C., Luppen, C.A., Kim, J.B., DeBoer, A.T., Wei, K., Helms, J.A., Kuo, C.J., Kraft, D.L., and Weissman, I.L. (2009). Endochondral ossification is required for haematopoietic stem-cell niche formation. Nature *457*, 490–494.

Christensen, J.L., Wright, D.E., Wagers, A.J., and Weissman, I.L. (2004). Circulation and chemotaxis of fetal hematopoietic stem cells. PLoS Biol. *2*, E75.

Ding, L., and Morrison, S.J. (2013). Haematopoietic stem cells and early lymphoid progenitors occupy distinct bone marrow niches. Nature *495*, 231–235.

Ding, L., Saunders, T.L., Enikolopov, G., and Morrison, S.J. (2012). Endothelial and perivascular cells maintain haematopoietic stem cells. Nature *481*, 457–462.

Greenbaum, A., Hsu, Y.M., Day, R.B., Schuettpelz, L.G., Christopher, M.J., Borgerding, J.N., Nagasawa, T., and Link, D.C. (2013). CXCL12 in early mesenchymal progenitors is required for haematopoietic stem-cell maintenance. Nature *495*, 227–230.

Kronenberg, H.M. (2003). Developmental regulation of the growth plate. Nature *423*, 332–336.

Madisen, L., Zwingman, T.A., Sunkin, S.M., Oh, S.W., Zariwala, H.A., Gu, H., Ng, L.L., Palmiter, R.D., Hawrylycz, M.J., Jones, A.R., et al. (2010). A robust and high-throughput Cre reporting and characterization system for the whole mouse brain. Nat. Neurosci. *13*, 133–140.

Maes, C., Kobayashi, T., Selig, M.K., Torrekens, S., Roth, S.I., Mackem, S., Carmeliet, G., and Kronenberg, H.M. (2010). Osteoblast precursors, but not mature osteoblasts, move into developing and fractured bones along with invading blood vessels. Dev. Cell *19*, 329–344.

Méndez-Ferrer, S., Michurina, T.V., Ferraro, F., Mazloom, A.R., Macarthur, B.D., Lira, S.A., Scadden, D.T., Ma'ayan, A., Enikolopov, G.N., and Frenette, P.S. (2010). Mesenchymal and haematopoietic stem cells form a unique bone marrow niche. Nature *466*, 829–834.

Mignone, J.L., Kukekov, V., Chiang, A.S., Steindler, D., and Enikolopov, G. (2004). Neural stem and progenitor cells in nestin-GFP transgenic mice. J. Comp. Neurol. *469*, 311–324.

Mizoguchi, T., Ahmed, J., Kunisaki, Y., Pinho, S., Ono, N., Kronenberg, H.M., and Frenette, P.S. (2014). Osterix marks distinct waves of primitive and definitive stromal progenitors during bone marrow development. Dev. Cell *29*, this issue, 340–349.

Mokrý, J., Cízková, D., Filip, S., Ehrmann, J., Osterreicher, J., Kolár, Z., and English, D. (2004). Nestin expression by newly formed human blood vessels. Stem Cells Dev. *13*, 658–664.

Nagasawa, T., Hirota, S., Tachibana, K., Takakura, N., Nishikawa, S., Kitamura, Y., Yoshida, N., Kikutani, H., and Kishimoto, T. (1996). Defects of B-cell lymphopoiesis and bone-marrow myelopoiesis in mice lacking the CXC chemokine PBSF/SDF-1. Nature *382*, 635–638.

Nakamura, E., Nguyen, M.T., and Mackem, S. (2006). Kinetics of tamoxifen-regulated Cre activity in mice using a cartilage-specific CreER(T) to assay temporal activity windows along the proximodistal limb skeleton. Dev. Dyn. *235*, 2603–2612.

Otto, F., Thornell, A.P., Crompton, T., Denzel, A., Gilmour, K.C., Rosewell, I.R., Stamp, G.W., Beddington, R.S., Mundlos, S., Olsen, B.R., et al. (1997). Cbfa1, a candidate gene for cleidocranial dysplasia syndrome, is essential for osteoblast differentiation and bone development. Cell *89*, 765–771.

Ovchinnikov, D.A., Deng, J.M., Ogunrinu, G., and Behringer, R.R. (2000). Col2a1-directed expression of Cre recombinase in differentiating chondrocytes in transgenic mice. Genesis *26*, 145–146.

Rodda, S.J., and McMahon, A.P. (2006). Distinct roles for Hedgehog and canonical Wnt signaling in specification, differentiation and maintenance of osteoblast progenitors. Development *133*, 3231–3244.

Sacchetti, B., Funari, A., Michienzi, S., Di Cesare, S., Piersanti, S., Saggio, I., Tagliafico, E., Ferrari, S., Robey, P.G., Riminucci, M., and Bianco, P. (2007). Self-renewing osteoprogenitors in bone marrow sinusoids can organize a hematopoietic microenvironment. Cell *131*, 324–336.

St-Jacques, B., Hammerschmidt, M., and McMahon, A.P. (1999). Indian hedgehog signaling regulates proliferation and differentiation of chondrocytes and is essential for bone formation. Genes Dev. *13*, 2072–2086.

Sugiyama, T., Kohara, H., Noda, M., and Nagasawa, T. (2006). Maintenance of the hematopoietic stem cell pool by CXCL12-CXCR4 chemokine signaling in bone marrow stromal cell niches. Immunity *25*, 977–988.

Szabova, L., Yamada, S.S., Wimer, H., Chrysovergis, K., Ingvarsen, S., Behrendt, N., Engelholm, L.H., and Holmbeck, K. (2009). MT1-MMP and type II collagen specify skeletal stem cells and their bone and cartilage progeny. J. Bone Miner. Res. *24*, 1905–1916.

Teranishi, N., Naito, Z., Ishiwata, T., Tanaka, N., Furukawa, K., Seya, T., Shinji, S., and Tajiri, T. (2007). Identification of neovasculature using nestin in colorectal cancer. Int. J. Oncol. *30*, 593–603.

Wroblewski, J., Engström, M., Edwall-Arvidsson, C., Sjöberg, G., Sejersen, T., and Lendahl, U. (1997). Distribution of nestin in the developing mouse limb bud in vivo and in micro-mass cultures of cells isolated from limb buds. Differentiation *61*, 151–159.

Zhang, J., Niu, C., Ye, L., Huang, H., He, X., Tong, W.G., Ross, J., Haug, J., Johnson, T., Feng, J.Q., et al. (2003). Identification of the haematopoietic stem cell niche and control of the niche size. Nature *425*, 836–841.